

<https://doi.org/10.1038/s41746-025-01678-z>

# Seasonal timing and interindividual differences in shiftwork adaptation

Ruby Kim<sup>1</sup>✉, Yu Fang<sup>2</sup>, Minki Lee<sup>1</sup>, Dae Wook Kim<sup>1,3</sup>, Zhengxu Tang<sup>1</sup>, Srijan Sen<sup>2,4</sup> & Daniel B. Forger<sup>1,5</sup>✉

Millions of shift workers in the U.S. face an increased risk of depression, cancer, and metabolic disease, yet individual responses to shift work vary widely. We find that a conserved biological system of morning and evening oscillators, which evolved for seasonal timing, may contribute to these interindividual differences. In this study, we analyze seasonality in medical interns working shifts, revealing that summer-winter variation correlates with increased circadian misalignment after shift work. Mathematical modeling suggests that seasonal timing influences the rate of adaptation to new schedules, predicting differential effects on morning and evening oscillators. Additionally, we examine genetic polymorphisms linked to seasonality in animals and find that human variants can impact how quickly circadian rhythms respond to schedule changes. Based on our findings, we hypothesize that the vast interindividual differences in shift work adaptation—critical for shift worker health—can in part be explained by biological mechanisms for seasonal timing.

Daily biological functions such as sleep, heart rate and metabolism are timed by intracellular circadian clocks which exist within almost all cells throughout the body. Modern life challenges this timekeeping system in ways it was not adapted for. Industrialization, shift work, indoor lighting, and smartphones drastically affect our sleep and the circadian timing of our biological systems<sup>1,2</sup>. We are only beginning to understand the implications for how these factors affect human health. A tremendous amount of evidence from plant and animal studies suggests that this timing is photoperiodic and requires a multi-oscillator system<sup>3,4</sup>. Thus, organisms anticipate at least both dawn and dusk, rather than a single time of day. Substantial evidence from human studies show that photoperiod alone can drive seasonal activity<sup>5,6</sup>. Much of this photoperiodism is coordinated intracellularly in plants<sup>7</sup> whereas animals such as *Drosophila* and mice time dawn and dusk using a system of “evening” and “morning” oscillators that were studied by Pittendrigh and Daan almost 50 years ago<sup>8</sup>. There is strong evidence for this dual oscillator framework across species, from splitting behavior in diurnal rodents<sup>9</sup> to bimodal activity in *Drosophila*<sup>10</sup>. The suprachiasmatic nucleus (SCN) within the brain, often referred to as the “central circadian pacemaker,” has multiple cell types which express different genes and synchronizing agents such as vasoactive intestinal polypeptide (VIP), neuromedin-S (NMS), and arginine vasopressin (AVP)<sup>11</sup>. Many aspects of circadian timekeeping are conserved across species, including the transcription-translation feedback loop structure<sup>12</sup> and metabolic activity in the SCN<sup>13</sup>. Overall, there is tremendous support in the

literature that multiple oscillators control circadian timing across species, including in humans<sup>14,15</sup>.

This multi-oscillatory timing of dawn and dusk has largely been ignored in the human circadian rhythms literature. However, a careful look at the data suggests that it could be quite important. Laboratory studies have shown that human sleep duration and melatonin profiles vary according to photoperiod<sup>6,16</sup>, and these effects are pronounced in seasonal affective disorder (SAD)<sup>17</sup>. In controlled settings, photoperiod also affects body temperature, prolactin secretion, and cortisol secretion<sup>6</sup>. When humans are exposed to natural lighting conditions, their melatonin rhythms encode dawn and dusk<sup>18</sup>. With the advancement and increasing prevalence of wrist wearable technology, there is growing evidence in support of photoperiodic encoding in our day-to-day lives. Bedtimes and wake times vary significantly throughout the year<sup>19,20</sup> and significant but modest changes in sleep duration were observed in ref. 20. In another study<sup>21</sup>, sleep duration in over 68,000 participants in Japan increased about 40 min from summer to winter on average. A review paper analyzing data from 110 articles with over 100,000 participants shows that there are significant differences in physical activity and sedentary behavior across seasons<sup>22</sup>. The circadian clock seems to play a significant role in seasonal rhythms in weight gain<sup>23</sup>. Despite all the evidence for human seasonality, the detailed underlying mechanisms and role in day-to-day health have yet to be identified.

The Intern Health Study (IHS) is an annual cohort study that follows first-year medical residents in the U.S. for the whole intern year. The study

<sup>1</sup>Department of Mathematics, University of Michigan, Ann Arbor, MI, 48109, USA. <sup>2</sup>Michigan Neuroscience Institute, University of Michigan, Ann Arbor, MI, 48109, USA. <sup>3</sup>Department of Brain and Cognitive Sciences, KAIST, Daejeon, 34141, Republic of Korea. <sup>4</sup>Eisenberg Family Depression Center, University of Michigan, Ann Arbor, MI, 48109, USA. <sup>5</sup>Department of Computational Medicine and Bioinformatics, University of Michigan, Ann Arbor, MI, USA. ✉e-mail: [rshkim@umich.edu](mailto:rshkim@umich.edu); [forger@umich.edu](mailto:forger@umich.edu)

collects measurements of step count, sleep, and heart rate from wrist wearable devices during the study period. We study data from over 3000 medical interns in the U.S. in the 2017–2019 cohorts working both day and night shifts and find strong evidence of seasonal variation in activity and sleep duration. Using a validated digital biomarker of circadian rhythms of heart rate (HR)<sup>24–26</sup>, we study the misalignment between HR circadian rhythms and sleep-wake patterns. Studying medical interns on shifts, we find that individuals have drastically different circadian behaviors when adapting to night shifts, even if they behave similarly under typical conditions. In particular, we find that individuals with stronger seasonal encoding are more sensitive to frequent shift changes and have more HR-sleep misalignment on average.

Nurses' sleep schedules show similar inter-individual differences, which have been linked to genetic polymorphisms<sup>27</sup>. In addition, several recent genome-wide association studies (GWAS) have linked certain single nucleotide polymorphisms (SNPs) to sleep behaviors and circadian amplitude inferred from wearable devices<sup>28,29</sup>. However, the role of genetic polymorphisms in human seasonality is poorly understood. A previous GWAS study of SAD failed to identify any significant associations<sup>30</sup>, possibly due to the relatively small sample size (1380 cases and 2937 controls). Complex traits are often associated with combined effects of multiple SNPs, and many studies do not account for these interactions<sup>31</sup>. However, there is growing evidence that genetic factors do indeed affect seasonality<sup>32</sup>.

A recent study found that the *SLC20A2* gene, which encodes sodium-dependent phosphate transporter 2 (PiT2), is expressed in VIP/NMS neurons localized in the SCN core and is involved in seasonality in mice<sup>33</sup>. *SLC20A2*-deleted mice failed to adapt to winter photoperiods, although they showed normal behavior with summer photoperiods and in response to phase shifts. Thus, we wondered if *SLC20A2* polymorphisms would influence human behavior observed throughout the year. In this study, we find that combinations of multiple SNPs of *SLC20A2* have statistically significant associations with altered physical activity, sleep duration, and circadian entrainment across seasons in the medical interns. We create a mathematical model of seasonal encoding in humans based on the dual circadian oscillator hypothesis by Pittendrigh and Daan<sup>8</sup> to study inter-individual differences in seasonal behavior explained by differences in neural coupling in different parts of the SCN. Our model predicts that certain individuals have quicker circadian entrainment than others, surprisingly causing more circadian misalignment on average in the context of shift work. Overall, our work demonstrates that seasonal timing mechanisms may play a significant role in shiftwork adaptation and contribute to the large inter-individual variability in daily behavior found in the data.

## Results

### Seasonal variation in daily activity and time awake

We analyzed wrist-wearable step data between May 2017 and March 2020 from over 3000 participants of the IHS (Fig. 1a). The geographic locations of these participants were spread out across the U.S. with latitudes ranging from 21.3°N to 48°N (Fig. 1b). In line with previous studies<sup>22</sup>, we found that the medical interns had significant variation in daily steps throughout the year with the largest daily steps in the summer ( $8453.67 \pm 60.03$  (SEM) steps) and lowest in the winter ( $7588.75 \pm 69.33$  (SEM) steps) (Fig. 1c). The data were binned by meteorological season (months 3–5 as Spring, 6–8 Summer, 9–11 Fall, and 12, 1, 2 Winter) and compared via one-way ANOVA ( $F(3,7309) = 28.95, p = 1.33 \times 10^{-18}, \eta^2 = 0.0117$ ) with Tukey's test. Traditionally, seasonality has been studied in terms of activity duration—the dual oscillator model by Pittendrigh and Daan<sup>8</sup> posits that length of activity changes with photoperiod. Accordingly, we determined long intervals of time awake from minute-level sleep data collected by the wearable devices for each participant. All durations of time awake (sleep=0 for each minute) between 6 and 24 h in length were recorded as time awake for the corresponding date. We chose 6 h as a reasonable lower bound to exclude short wake periods within sleep sessions. We found that time awake in the medical interns varied significantly across seasons as well, with longer periods of time awake in the summer ( $15.83 \pm 0.04$  (SEM) hours) than in the winter

( $15.52 \pm 0.06$  (SEM) hours) or spring ( $15.54 \pm 0.08$  (SEM) hours), though the effect size was small (Fig. 1e, one-way ANOVA,  $F(3,2019) = 6.43, p = 2.47 \times 10^{-4}, \eta^2 = 0.0095$ ; with Tukey's test). This finding corroborates previous studies<sup>20,21</sup> showing seasonal patterns in sleep duration. Activity across the year is influenced by many external factors, yet we see statistically significant effects of seasons with highest activity in the summer.

While time awake is an important behavioral endpoint of seasonality, the size of the sleep data was small compared to the step data (87,600 data points across all participants, compared to 355,744 for steps). Based on the data, the wearable devices were not worn consistently during sleep. However, we found that time awake was strongly associated with daily steps (Fig. 1d, linear regression coefficient  $\beta_1 = 549.42, p = 5.36 \times 10^{-155}$ ), indicating that large step counts were likely spread out over long periods of time awake. As a result, we chose to use daily steps as our main behavioral endpoint of interest in favor of statistical power. The difference in daily steps between summer and winter was strongly associated with latitude (Fig. 1f, linear regression coefficient  $\beta_1 = 32.3221, p = 6.02 \times 10^{-3}$ ). Based on the length of day model from<sup>34</sup>, the photoperiod varies as little as 2.1 h or as much as 8.2 h throughout the year, depending on the participants' latitude.

### Dual oscillator model for seasonal encoding

Based on the notable seasonal variation we found in activity and circadian rhythms, we decided to explore the potential mechanisms underlying seasonal behavior and responses to shift work using a dual oscillator framework as proposed by Pittendrigh and Daan<sup>8</sup>. The model in this paper consists of two ordinary differential equations (ODEs) describing the rate of change of the phases of two oscillator populations, the evening (E) and morning (M) oscillators. The oscillator populations are coupled to each other and to a light signal, where synchronization rates depend sinusoidally on the phase difference with the synchronizing oscillator (E, M, or light). A schematic diagram is provided in Fig. 2a, and the ODEs are given in the Methods.

In simulations, when the photoperiod is increased from 8 h to 16 h, the phase gap between the two oscillators also increases (Fig. 2b). We took this model phase gap to represent activity, as in Pittendrigh and Daan's study<sup>8</sup>. Our model has 7 parameters: two are related to light signaling in the evening oscillator ( $a_e, b_e$ ), two are related to light signaling in the morning oscillator ( $a_m, b_m$ ), two are the coupling strengths between the two oscillators ( $A_M, A_E$ ), and one is related to the oscillators' intrinsic frequencies ( $p$ ). The parameters are described further in the Methods.

Following Pittendrigh and Daan<sup>8</sup>, we simulated actograms using our mathematical model (Fig. 2c). Shaded regions indicate 5-hour time periods starting from oscillator peaks, to visualize the circadian clock's influence on activity. We ran simulations with a 12:12 light-dark cycle, then every 30 days we adjusted the light-dark schedule either by introducing 3-hour phase shifts (Fig. 2c, left), changing the photoperiod (Fig. 2c, center)—from 12 h to 20 h, back to 12 h, and finally down to 4 h for the last 30 days, or by shifting the light-dark schedule by 12 h (Fig. 2c, right). After 3-hour phase shifts, the solutions take some time to re-entrain to the new schedule, but the phase gap between the E and M oscillators stays consistent during the entrainment periods. When the photoperiod is lengthened, the E and M oscillators gradually move apart in phase, and when the photoperiod is shortened, the phases of the oscillators gradually get closer. Interestingly, a 12 h phase shift can produce splitting behavior similar to that seen in animal studies<sup>15</sup>. The phases of the E and M oscillators gradually grow apart until they switch places relative to the new schedule, cross each other, and then become fully re-entrained. This behavior depends on parameters, which we discuss later.

### Seasonality and shiftwork adaptation

There are various circadian rhythms throughout the body that can be misaligned with each other<sup>35</sup>. For example, it is known that heart rate is generally lowest during sleep<sup>36</sup>, but the circadian rhythms of heart rate can be out of phase with the sleep-wake cycle, and this internal misalignment has been associated with an increased risk of cardiovascular disease<sup>37</sup> and mental health risks<sup>38,39</sup>. For some individuals heart rate is lowest early during the sleep period, and for others it reaches its minimum later<sup>39</sup>. In our data on

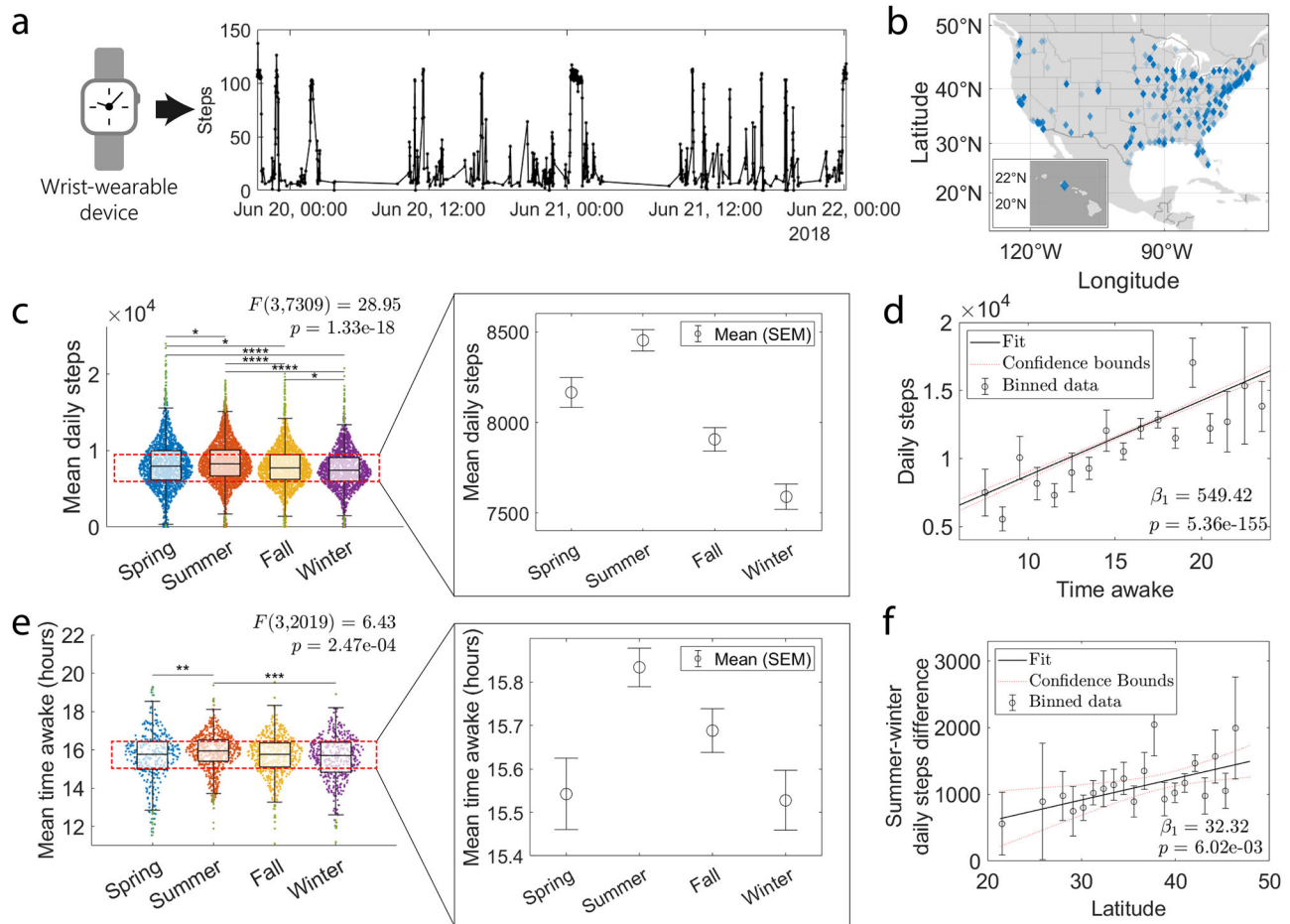


**Fig. 1 | Daily activity varies seasonally according to latitude.** **a** Step data across the year-long internship is collected through a wrist-wearable device. **b** Geographic coordinates of study participants, with latitudes varying from 21.3°N to 48°N. **c** Mean daily steps binned by meteorological seasons Spring ( $n = 1709$ ), Summer ( $n = 2280$ ), Fall ( $n = 1841$ ), and Winter ( $n = 1483$ ) (one-way ANOVA,  $F(3,7309) = 28.95$ ,  $p = 1.33 \times 10^{-18}$ ,  $\eta^2 = 1.17 \times 10^{-2}$ ; with Tukey's test,  $*p < 0.05$ ,  $***p < 1 \times 10^{-4}$ ). **d** Daily steps are strongly associated with time awake (linear regression coefficient  $\beta_1 = 549.42$ ,  $p = 5.36 \times 10^{-155}$ , adjusted  $R^2 = 81 \times 10^{-3}$ ). The model is fit to individual data ( $n = 86,536$  across 673 subjects) and plotted in bins for

easier visualization. Error bars are standard error of the mean. **e** Mean daily time awake binned by meteorological seasons Spring ( $n = 342$ ), Summer ( $n = 672$ ), Fall ( $n = 564$ ), and Winter ( $n = 445$ ) (one-way ANOVA,  $F(3,2019) = 6.43$ ,  $p = 2.47 \times 10^{-4}$ ,  $\eta^2 = 9.5 \times 10^{-3}$ ; with Tukey's test,  $**p < 0.01$ ,  $***p < 1 \times 10^{-3}$ ). **f** Mean daily steps during the summer minus mean daily steps during the winter for each participant ( $n = 1471$ ) plotted against their latitude (linear regression coefficient  $\beta_1 = 32.3221$ ,  $p = 6.02 \times 10^{-3}$ , adjusted  $R^2 = 4.5 \times 10^{-3}$ ). Error bars are the standard error of the mean.

average HR minimum occurs around  $0.45 \pm 5.64$  (SD) hours before sleep midpoint. Not only is the phase relationship between the two rhythms highly variable from individual to individual, but it also varies widely within individuals.

We used the Bowman algorithm<sup>24</sup> to extract circadian phase from HR data. The algorithm uses a 24-hour sinusoidal model with a likelihood-based approach that is not significantly affected by large intervals of missing data. More details are provided in the Methods. We took the absolute difference between HR circadian phase or minimum ( $HR_{min}$ ) and sleep midpoint ( $SM$ ) measured by the wearable devices to compute a metric we call "HR-sleep misalignment." In other words,  $HR\text{-}sleep\text{ misalignment} = \min(|HR_{min} - SM|, 24 - |HR_{min} - SM|)$  (Fig. 3a). The distributions of  $HR_{min}$ ,  $SM$ , and HR-sleep misalignment are shown in Fig. 3b. We generally expect the HR minimum to be close to the sleep midpoint, so that misalignment is close to zero. There are two bumps in the distributions of  $HR_{min}$  and  $SM$  because the participants are on night shifts for a small fraction of the internship year. HR-sleep misalignment is much higher on average during "night schedules," when the sleep midpoint is between 12:00 and 24:00 (Fig. 3c).  $HR_{min}$  and  $SM$  can change from day to day, especially as individuals are switching between different shift schedules. For example, the HR circadian phase along with step actograms of two different participants are plotted in Fig. 3d.

Some participants had reduced seasonal variation in activity, with little to no difference between summer and winter step counts. Others (23.5% of participants) had the opposite behavior from most participants, with more steps during the winter than during the summer, possibly indicating that these individuals were more responsive to other seasonal rhythms (e.g., hospital burden) rather than photoperiod. We found that participants with larger summer-winter differences in daily steps, with more activity during the summer than in the winter, were more likely to have higher HR-sleep misalignment after winter night shift work (Fig. 3f). Data were averaged across all days immediately following night shifts for each participant, regardless of the shift schedule following the night shift. The correlation between HR-sleep misalignment after night shifts and summer-winter steps differences was not found during the summer (Fig. 3e). The data suggest that individuals with larger seasonal variation in activity are more likely to experience circadian misalignment after night shifts in the winter than individuals with reduced or no seasonal variation. On the night shift days, there wasn't a significant association between HR-sleep misalignment and summer-winter steps differences in the summer ( $n = 1,786$ ,  $\beta_1 = 2.40 \times 10^{-5}$ ,  $p = 4.56 \times 10^{-1}$ ) or winter ( $n = 1,254$ ,  $\beta_1 = 6.36 \times 10^{-5}$ ,  $p = 1.01 \times 10^{-1}$ ), not pictured. In addition, we also found that summer-winter daily steps differences were significantly associated with average absolute daily changes in

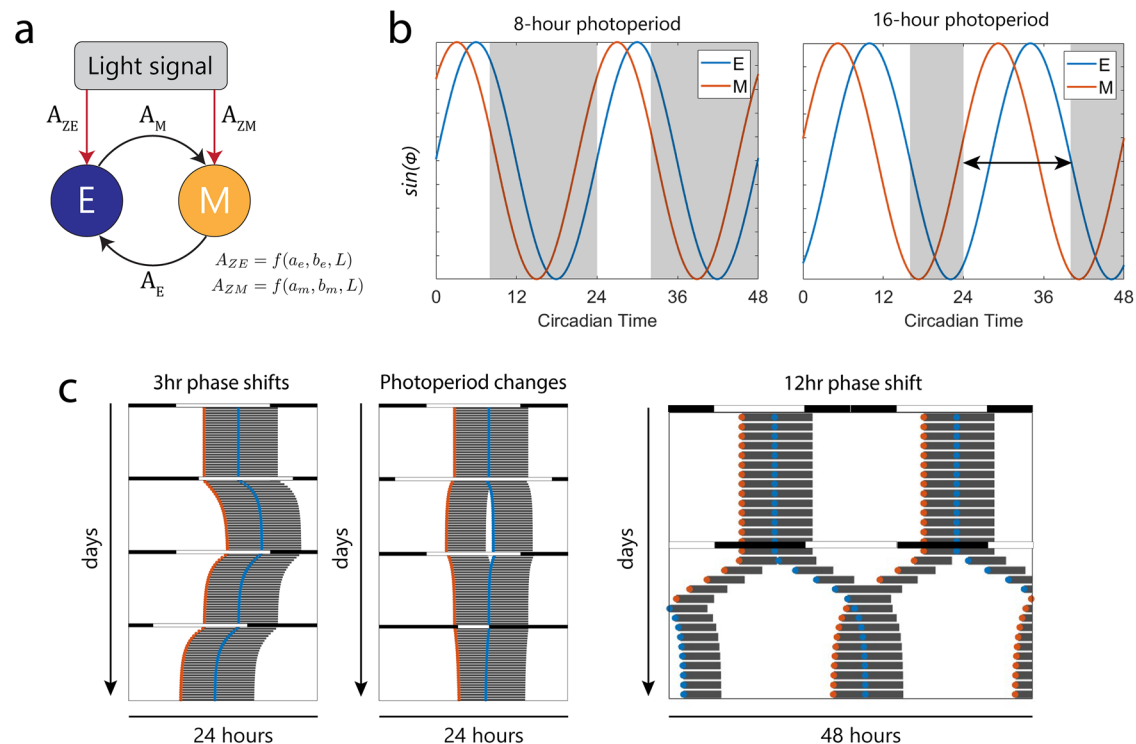


**Fig. 2 | Dual oscillator model for seasonal encoding.** **a** Schematic of dual oscillator model for circadian timekeeping in the SCN. In this paper, the evening (E) and morning (M) oscillators are modeled as coupled phase oscillators which both receive light signaling. **b** The phase gap between the E and M oscillators increases to adapt to long photoperiods. **c** Model actograms using nominal parameter values. The shaded regions start at the peaks of  $\sin(\phi_E)$  and  $\sin(\phi_M)$  and span 5 h as in ref. 8. From left to

right, we simulate 3-hour phase shifts, photoperiod changes, and a 12-hour phase shift. For the 3-hour phase shifts, the 12:12 light-dark schedule is delayed or advanced by 3 h (left). To simulate photoperiod changes, the photoperiod is increased to 20 h, then decreased back to 12 h, then reduced to 4 h (center). To simulate night shift work, the schedule is shifted by 12 h (right).

HR circadian phase (Supplementary Fig. 1), indicating that individuals with larger summer-winter variation were more likely to have larger day-to-day variation in HR phase. As we will discuss later, the effects of night shift work on HR circadian phase were typically not observed until a day after the night shifts.

### Combined effects of *SLC20A2* SNPs

A recent animal study<sup>33</sup> shows that the *SLC20A2* gene is involved in seasonality in mice, but the effects of the gene on seasonality in humans have not been studied. From the 225,466 variants genotyped in our sample, we found 6 single-nucleotide polymorphisms (SNPs) of *SLC20A2* (rs3763510, rs34749433, rs4737046, rs6988483, rs13281070, and rs7818789). We checked for linkage disequilibrium (LD) and found that the SNPs were independent except for rs7818789, which we excluded from our study. We then studied the combined effects of the remaining 5 SNPs. For each SNP, we chose the allele with the highest frequency as the reference allele, and encoded the genotype for each SNP as 0, 1, or 2 for homozygous non-reference, heterozygous, and homozygous reference, respectively. As a result, each participant's *SLC20A2* genotype was represented by a 5-dimensional vector with elements 0, 1, or 2. In our sample, there were 79 different genotype combinations. Only 23.4% of medical interns who provided genomic data have the homozygous reference genotype [2,2,2,2,2] for all 5 SNPs. The most common genotype combination was<sup>1,2</sup> in 26% of the subjects. In this study, we refer to the 10 most common genotype combinations as groups 1–10 and compare daily steps and HR-sleep misalignment across the 10 genotype groups; group percentages are visualized in Fig. 4a. The numbers of individuals in each group were:  $n = 1271$  for group 1,  $n = 1137$  for group 2,  $n = 416$  for group 3,  $n = 391$  for group 4,  $n = 372$  for group 5,  $n = 298$  for group 6,  $n = 294$  for group 7,  $n = 259$  for group 8,  $n = 226$  for group 9, and  $n = 194$  for group 10. We did not analyze any

further genotype groups due to small sample sizes. Across all individuals in the 10 genotype groups, we had  $20.33 \pm 5.81$  (SD) hours of minute-level heart rate data on average per day and  $219.48 \pm 112.42$  (SD) days of heart rate data per person on average.

We conducted generalized estimating equation (GEE) analyses for daily steps, time awake, and HR-sleep misalignment to investigate the effects of genotype while accounting for the correlation of within-subject data. We considered the following 12 input variables for each analysis: genotype group, day of year, and the top 10 genotype-based principal components (PCs) using the MATLAB toolbox GEEQBOX<sup>40</sup>. Principal components analysis was used to help adjust for population stratification<sup>41</sup>. We assumed an autoregressive (Lag 1) (AR(1)) correlation structure where correlations are highest between adjacent times. We found that genotype group is a significant predictor of daily steps, time awake, and HR-sleep misalignment. We then conducted pairwise GEE analyses with Bonferroni correction for the 45 comparisons across 10 groups and found that group 10 had the most significant pairwise differences ( $p < 0.05/45 \approx 0.0011$ ) from other groups in daily steps, group 1 had the most significant pairwise differences from other groups in time awake, and group 9 had the most significant pairwise differences from other groups in HR-sleep misalignment (Fig. 4b). The statistics for the GEE analyses across all 10 groups for daily steps, time awake, and HR-sleep misalignment, as well as for the 45 pairwise GEE models are provided in the supplementary materials.

The time courses of daily steps, HR-sleep misalignment, and time awake for groups 9 and 10 also show some qualitative differences from group 1 (Fig. 4d, f). While the peak of activity is in June for all three groups, the amplitude of seasonal variation in daily steps is larger on average in group 10 than in groups 1 and 9; see Fig. 4d. Seasonal variation of circadian misalignment between different endogenous clocks has previously been observed in ref. 42. The HR-sleep misalignment curve for group 9 has large



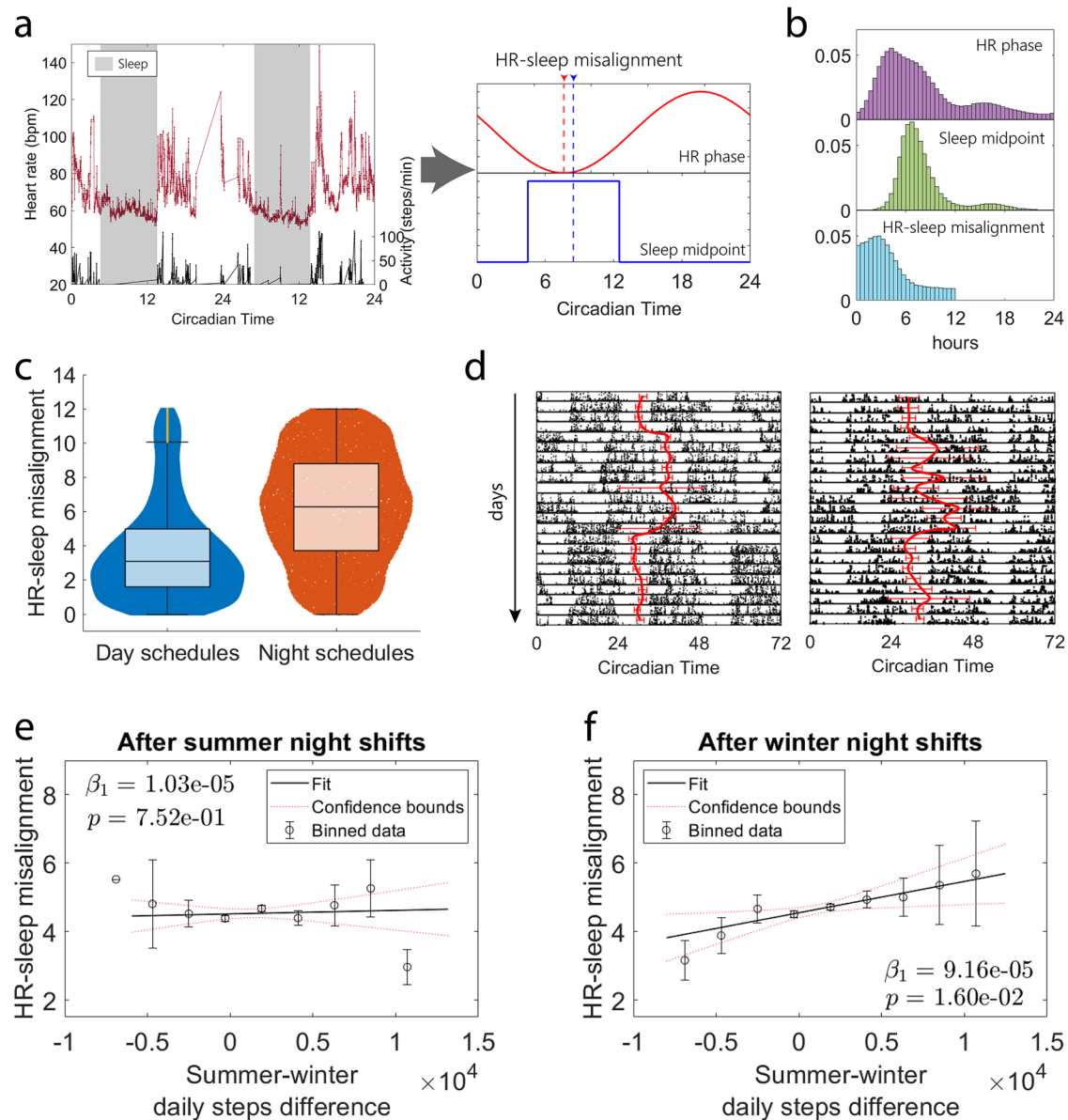


**Fig. 3 | HR-sleep misalignment due to night shift work is associated with summer-winter activity differences.** **a** Heart rate circadian phase, and sleep midpoint are measured from wrist-wearable data using previously validated methods<sup>24</sup>. HR-sleep misalignment is defined as the absolute difference between HR circadian phase and sleep midpoint. **b** Histograms for all participants for HR circadian phase (top), sleep midpoint (middle), and HR-sleep misalignment (bottom). There are small secondary bumps in HR phase and sleep midpoint because the participants are on night shifts for part of the program. **c** HR-sleep misalignment is much higher on average during night schedules, when the sleep midpoint is past 12:00. **d** Step actograms showing example activity for two different subjects. The red curve indicates HR circadian phase, and the error bars indicate 80% confidence bands. The

subject on the left adjusts to a new schedule within a few days, while the subject on the right has large day-to-day fluctuations in the HR circadian phase. **e** Mean HR-sleep misalignment after night shifts is not significantly associated with summer-winter daily steps difference during the summer (linear regression coefficient  $\beta_1 = 1.03 \times 10^{-5}$ ,  $p = 7.52 \times 10^{-1}$ ). The linear model is fit to individual data ( $n = 1618$ ), and the data are binned for easier visualization. Error bars are the standard error of the mean. **f** Mean HR-sleep misalignment after a schedule change is significantly associated with summer-winter daily steps difference during the winter (linear regression coefficient  $\beta_1 = 9.16 \times 10^{-5}$ ,  $p = 1.60 \times 10^{-2}$ , adjusted  $R^2 = 4.3 \times 10^{-3}$ ). The linear model is fit to individual data ( $n = 1138$ ), and the data are binned for easier visualization. Error bars are the standard error of the mean.

fluctuations, particularly in the spring. Groups 9 and 10 on average have more HR-sleep misalignment than group 1, especially in the winter; see Fig. 4e. To check for differences in shift work schedules that might contribute to the misalignment, we computed the fraction of night schedules where the sleep midpoint was between 12:00 and 24:00, which was around 5% on average, and found that there was no significant difference between groups (one-way ANOVA,  $F(9,1448) = 1.3044$ ,  $p = 0.2295$ ). Interestingly, we find that there is larger variation in HR-sleep misalignment across the genotype groups during the winter than during the summer (Fig. 4c). The standard deviation of the mean HR-sleep misalignment within genotype groups is

0.2979 during the winter and 0.1186 during the summer, which is significantly different with a Bartlett's Test  $p$ -value of  $p = 0.01145$ . Plotting time awake throughout the year, we see that the most common genotype group has relatively small changes in time awake throughout the year compared to the other two groups (Fig. 4f).

#### Altered seasonal timing and shiftwork adaptation in genotype groups

We used our mathematical model to study the potential mechanisms underlying the differences we found between the genotype groups. In the

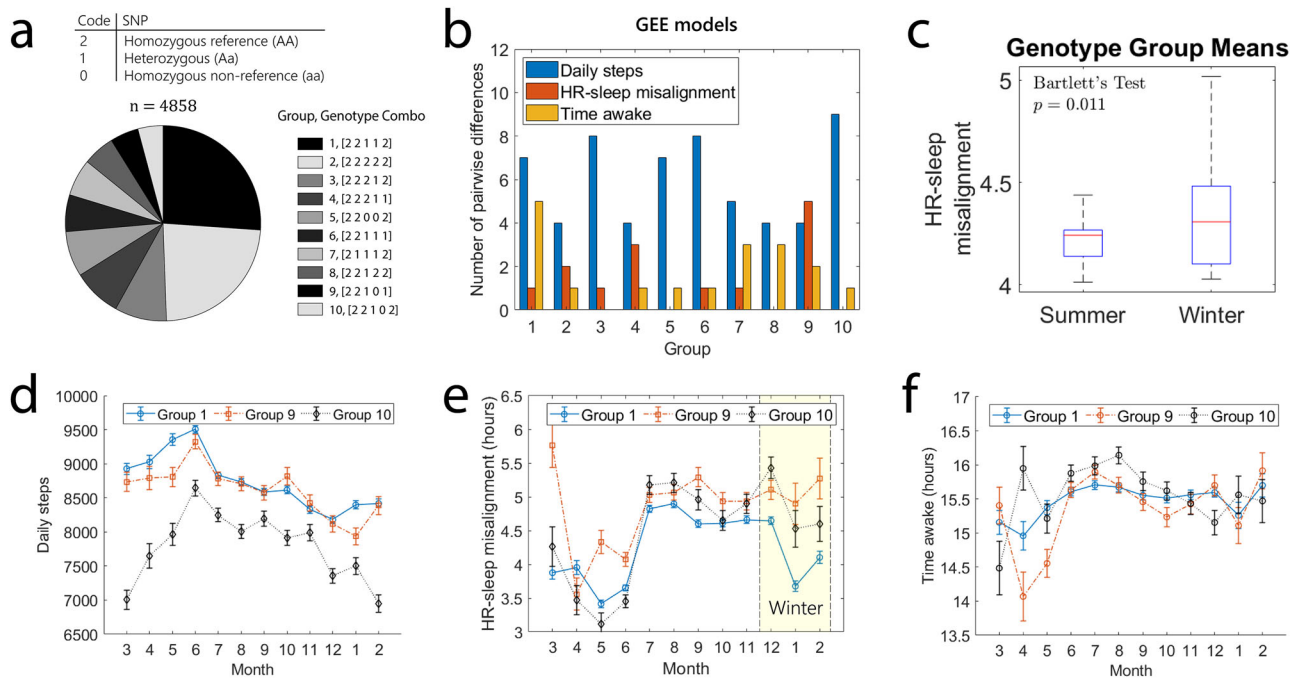


**Fig. 4 | Seasonal changes in *SLC20A2* polymorphism groups.** **a** Each subject's genotype is categorized by a 5-dimensional vector encoding the 5 *SLC20A2* SNPs. We encode each SNP with the value 2 (homozygous reference), 1 (heterozygous), or 0 (homozygous non-reference). The pie chart shows the 10 most common genotype combinations of the 5 SNPs. The 10 groups make up 76.44% of the subjects. **b** Differences between groups are tested using generalized estimating equation (GEE) models with day of year and the top 10 principal components (PCs) as covariates. There is a significant difference between groups for daily steps ( $p = 0.0014$ ), HR-sleep misalignment ( $p = 0.0082$ ), and time awake ( $p = 0.0206$ ). The bars visualize the number of significant pairwise differences ( $p < 0.0011$ ) for each of the 10 groups, using GEE analyses with Bonferroni correction. **c** Mean HR-sleep

misalignment calculated for each genotype group has a significantly larger variance during the winter than during the summer (Bartlett's Test,  $p = 0.011$ ). **d** Daily steps over the year for genotype groups 1, 9, and 10. Group 1 is the most common genotype group, and Groups 9 and 10 have the most pairwise differences from the other groups in HR-sleep misalignment and daily steps, respectively, shown in panel (b). Error bars are the standard error of the mean. **e** HR-sleep misalignment for groups 1, 9, and 10. Error bars are the standard error of the mean. HR-sleep misalignment is visibly different across the three groups, especially during the winter. **f** Time awake for groups 1, 9, and 10. Error bars are the standard error of the mean. Time awake in group 1 has a smaller amplitude of change compared to the other two groups.

ODE model, the parameters  $a_e$ ,  $a_m$ ,  $b_e$ , and  $b_m$  adjust coupling of the evening (subscript 'e') and morning (subscript 'm') oscillators to light signaling, the parameters  $A_M$  and  $A_E$  are the coupling strengths between the two oscillators, and  $p$  adjusts the separation of intrinsic frequencies of the oscillators. We fit the 7 parameters and normalized model phase gap ( $\text{phase gap} = \min(|\phi_E - \phi_M|, 24 - |\phi_E - \phi_M|)$ ) to normalized daily steps data for each subject across all 10 groups. The ODE solutions and steps data were normalized by their respective means in group 1, and data were fit using the nonlinear least-squares fitting function *lsqnonlin* in MATLAB. Solutions were accepted for positive *exitflag*, which typically indicates a local solution was found. The same initial conditions, informed by previous studies<sup>43,44</sup>, were used across all subjects. After parameter fitting, outliers more than 3 scaled median absolute deviations (MAD) from the median were determined to be biologically unrealistic predictions of the parameters. More details for these modeling choices can be found in the Methods. An example of a model fit is provided in Fig. 5a. We performed one-way ANOVAs for all 7 parameters across all 10 groups and found significant differences between groups for only two parameters:  $a_e$ , which controls light signaling to the evening oscillator, and  $A_M$ , which controls E to M coupling; see Fig. 5b, c. Interestingly, we found that group 10 had significantly reduced  $a_e$  compared to group 1 (post-hoc Tukey's test,  $p = 0.0476$ ) and group 9 had significantly elevated  $A_M$  compared to groups 1-3 (post-hoc Tukey's test,  $p = 0.0129$ ,  $p = 0.0371$ ,  $p = 0.0437$ , respectively). There were no significant differences between groups for the remaining 5 parameters.

Within the dual oscillator framework, our model suggests that *SLC20A2* polymorphisms can control coupling between SCN regions or to light signals. *SLC20A2* is expressed in VIP/NMS neurons in the SCN, encoding a phosphate transporter that potentially influences signaling

pathways<sup>33</sup>. Groups 9 and 10 had altered HR-sleep misalignment and daily steps throughout the year in our GEE models. From the GEE models alone, it isn't clear why groups 9 and 10 have these differences. However, our ODE model suggests that these individuals have reduced coupling of the E oscillator to light ( $a_e$ , group 10) or increased E-to-M coupling ( $A_M$ , group 9). The effects of these parameters on circadian entrainment in the model are explored in Fig. 5d, e. While it's likely that a combination of multiple parameters drives individual differences in entrainment, contributing to the small observed effect sizes for each parameter in Fig. 5b, c, we focused on  $a_e$  and  $A_M$  because they showed statistically significant differences across genotype groups and we were interested in how changes in these parameters alone can influence entrainment patterns. These parameters represent coupling strengths, and though the precise mechanisms of coupling between SCN cells are not fully understood, they can reasonably vary by an order of magnitude<sup>45</sup>. With reduced coupling of the E oscillator to light ( $a_e$  reduced by a factor of 0.1), the M oscillator adjusts to new photoperiods quickly, while the E oscillator does not respond (Fig. 5d, left). With increased coupling from the E oscillator to M oscillator ( $A_M$  increased by a factor of 10), changes in response to photoperiod happen much more quickly in both directions (Fig. 5d, right). The effects of these parameter changes are much more noticeable in the case of a 12 h phase shift. In our study, the medical interns undergo night shifts for a small fraction of the year. Our model suggests that with reduced coupling of the E oscillator to light, entrainment to a 12 h phase shift happens much more slowly than in the nominal model (Fig. 5e, top, compared to Fig. 2c, right). With increased coupling from the E oscillator to M oscillator, circadian entrainment is quicker and there is no splitting behavior (Fig. 5e, bottom).

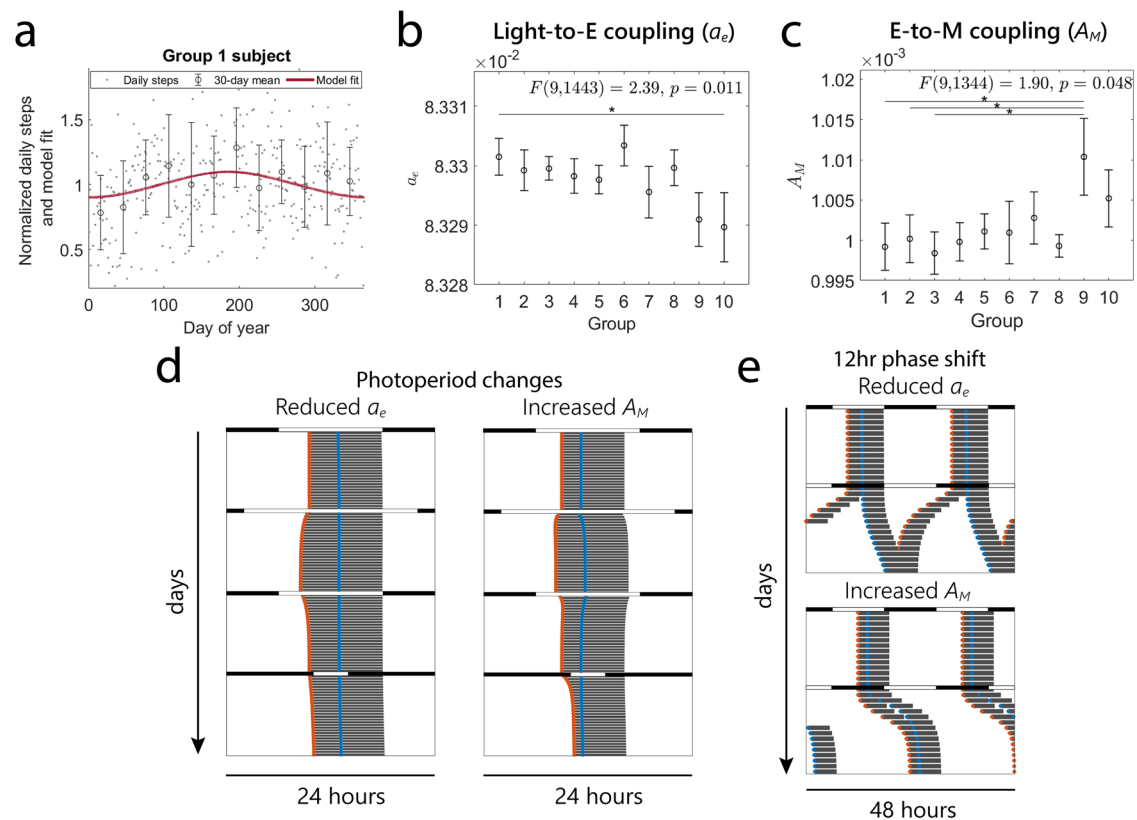


**Fig. 5 | Parameter fitting suggests altered seasonal tracking in polymorphism groups.** **a** Example of the ODE model fit to daily steps (gray points) data for a subject from Group 1. The 30-day means are plotted to help visualize the time course. Error bars indicate standard deviation. The phase gap computed by the ODE model and daily steps from the data are normalized by the respective group 1 means. **b**, **c** Two of the fitted parameters,  $a_e$  and  $A_M$ , are significantly different between the 10 genotype groups. **b** The parameter  $a_e$  adjusts coupling of the E oscillator to light signals. One-way ANOVA  $F(9, 1443) = 2.39$  and  $p = 0.011$ , with post-hoc Tukey's test,  $*p < 0.05$ , and  $\eta^2 = 0.0147$ . Error bars indicate standard error. On average, group 10 has smaller

$a_e$  than the other groups. **c** The parameter  $A_M$  determines the coupling from the E oscillator to the M oscillator. One-way ANOVA  $F(9, 1344) = 1.90$  and  $p = 0.048$ , with post-hoc Tukey's test,  $*p < 0.05$ , and  $\eta^2 = 0.0125$ . On average, group 9 has larger  $A_M$  than the other groups. **d** Model actograms for varying photoperiods with reduced coupling of the E oscillator to light ( $a_e$ ) and increased coupling from the E oscillator to M oscillator ( $A_M$ ). The shaded regions start at the peaks of  $\sin(\phi_E)$  and  $\sin(\phi_M)$  and span 5 h as in ref. 8. **e** Model actograms for a 12-hour light-dark schedule shift with reduced  $a_e$  (by a factor of 0.1) and increased  $A_M$  (by a factor of 10).

Based on our model, we predicted that group 9's intrinsic circadian rhythms would be more responsive to light signals and entrain more quickly than other groups. We investigated the dataset further, analyzing circadian entrainment and HR-sleep misalignment following night shifts, and found that the data indeed reflects the behavior predicted by our model. To study the effects of night shifts, we categorized them by whether they were isolated or happened consecutively (and how many times). We counted the number of isolated night shifts, the number of pairs of night shifts, the number of three consecutive night shifts, and so on, and found that the participants did not usually have more than two consecutive night shifts. 50% of the time night shifts were one-off and 32% of the time they were followed by a second night shift before returning to day shifts (Fig. 6b). With participants occasionally going on one or two night shifts, we found that there generally wasn't enough time for their HR circadian rhythms to change significantly. In the double-plotted actograms in Fig. 6a, we can see that the HR circadian phase seems to "ignore" occasional one-off night shifts. We note that the proportion of night shifts throughout the year was not significantly different across the 10 genotype groups (one-way ANOVA,  $p = 0.5465$ , not pictured).

We carefully studied the effects of single night shifts and two consecutive night shifts in the dataset and found that there were differences in entrainment rate and HR-sleep misalignment during and after the night shifts across genotype groups 1, 9, and 10. In these analyses, we considered night shifts that started after at least 30 days of day shifts. Previous studies suggest that entrainment to a night shift schedule could take anywhere from a few days to a few weeks<sup>46–48</sup>. The magnitude of the change in HR phase in response to the night shifts was larger in group 9 than in group 1, and as a

result group 9 had more HR-sleep misalignment during the day shifts that followed (Fig. 6c, d). We conducted one-way ANOVA analyses for each of the three groups' data across the four days. All 12 tests gave significant  $p$ -values, indicating statistically significant differences in the change in HR phase and HR-sleep misalignment across the days. There was relatively little change in the phase of HR rhythms of group 1 participants after a single night shift ( $-0.13 \pm 0.11$  (SEM) hours/day), so the HR-sleep misalignment was large on the days of the night shifts ( $7.22 \pm 0.13$  (SEM) hours). However, because the change in HR phase in response to night shifts was small, the HR-sleep misalignment in group 1 was relatively small in the following days after returning to day shifts ( $3.37 \pm 0.17$ ,  $3.44 \pm 0.18$ , and  $3.27 \pm 0.18$  (SEM) hours, for days 1–3). On the other hand, for group 9, because the change in HR phase in response to night shifts was large ( $-0.72 \pm 0.33$  (SEM) hours/day), although their HR-sleep misalignment was lower than that of other groups on the days of the night shifts ( $6.67 \pm 0.32$  (SEM) hours), their misalignment was relatively large after returning to day shifts ( $3.96 \pm 0.42$ ,  $4.29 \pm 0.40$ , and  $4.33 \pm 0.44$  (SEM) hours, for days 1–3); see Fig. 6c.

With two consecutive night shifts, we again see relatively large HR phase changes in group 9,  $1.75 \pm 0.71$  (SEM) hours/day on the second night shift compared to  $0.99 \pm 0.20$  (SEM) hours/day for group 1 (Fig. 6d). The data show a similar trend for three consecutive night shifts as well, with a HR-sleep misalignment of  $3.98 \pm 0.67$  (SEM) hours in group 9 and  $2.53 \pm 0.62$  (SEM) hours in group 1 immediately following 3 night shifts (not pictured). We repeated the analyses for single night shifts in the summer vs. winter, finding similar behaviors with larger HR phase changes and HR-sleep misalignment in group 9 compared to group 1 after the night

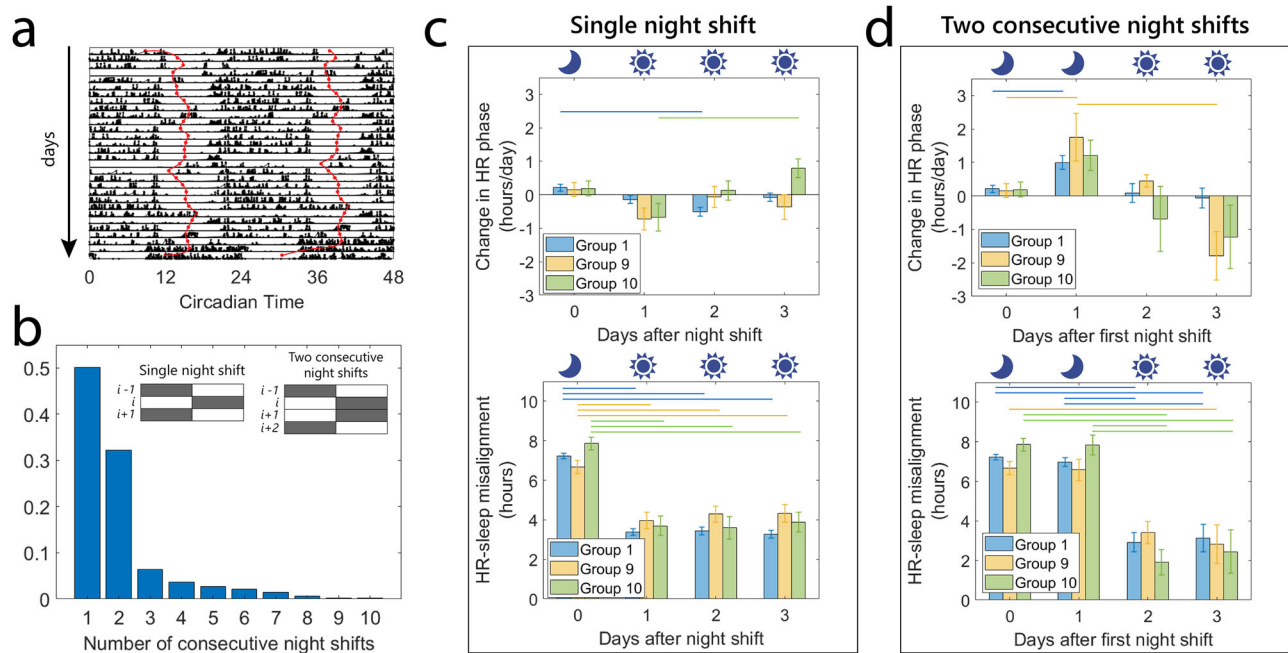


**Fig. 6 | Polymorphism group experiences quicker changes in HR circadian rhythms in response to night shifts.** **a** Example double-plotted actograms for a participant occasionally going on night shifts. The red curve indicates the phase of the HR circadian rhythms. **b** Frequency of number of consecutive night shifts. Most night shifts in the dataset were either isolated night shifts or two consecutive night shifts ( $n = 17,331$ ). **c** Change in HR phase (hours/day) and HR-sleep misalignment (hours) in response to a single night shift. Data are averaged across single night shifts that occur after at least 30 days of day shifts to help control for effects of previous shift schedules. The magnitude of the change in HR phase immediately after a single night shift is larger on average in groups 9–10 ( $-0.72 \pm 0.33$  (SEM) and  $-0.67 \pm 0.41$

(SEM) hours/day, respectively) than in group 1 ( $-0.13 \pm 0.11$  (SEM) hours/day). On average, group 9 has lower HR-sleep misalignment than group 1 on single night shift days but higher misalignment afterwards on days 1–3. Error bars indicate SEM. **d** Change in HR phase (hours/day) and HR-sleep misalignment (hours) in response to two consecutive night shifts. Group 9 responded with the largest change in HR phase on the second consecutive night shift (day 1, top). Group 9 had the most misalignment immediately after the two-night shifts (day 2, bottom). One-way ANOVA analyses for each of the three groups' data across the four days (for a total of 12 tests) all gave significant  $p$ -values. Horizontal lines indicate significant pairwise comparisons from post-hoc Tukey's tests.

shifts (Supplementary Fig. 2). Interestingly, the contrast in average behavior between groups was more dramatic in the winter. These observations align with our ODE model prediction that group 9 on average responds relatively quickly to night shifts. The data suggest that, while some individuals' circadian clocks might ignore occasional night shifts, group 9 is more sensitive to schedule changes and therefore can face more circadian misalignment over time.

## Discussion

In this study, we considered data from thousands of medical interns over their year-long internship. Due to the relative ease of collecting wrist-wearable data, we have the advantage of a large sample size. On the other hand, the data is not collected under controlled settings, so there is large variability due to external conditions: big life events, changes in diet, exposure to artificial lighting, etc. The main caveat with our study is that the participants are medical interns in non-laboratory settings, so the results must be interpreted carefully within this context. The medical interns in our study experience seasonal variation in activity, which could potentially be explained by many different environmental and social factors. Photoperiod and temperature often act as complementary environmental cues for seasonal behavior, where a decrease in day length generally coincides with a drop in temperatures, and significant effects of temperature have previously been demonstrated in other populations<sup>21,49</sup>. We believe that seasonal behavior is also influenced by occupational demands. It has been observed that hospital admissions typically increase in the winter, though it may depend on the type of care and medical conditions<sup>50–52</sup>. The highest activity in our dataset was typically in the summer, despite the potentially counteracting seasonal effects of hospital burden. We note that higher activity in the summer has been observed in other populations as well<sup>19–22</sup>, though the effect sizes in our study are

relatively small. Remarkably, we still find significant associations between seasonal behavior and shiftwork adaptation.

There is strong evidence in the literature that SAD is related to seasonal and circadian rhythms<sup>33</sup>. It is known that individuals with SAD are more likely to experience sleep problems<sup>54</sup>. In a previous study on medical interns participating in the IHS, we showed a bidirectional link between daily mood and circadian misalignment<sup>33</sup>. Future work could explore whether there is a seasonal component to this relationship, and whether this could provide clues about SAD or seasonal mood disorders. The focus of this study was to examine the relationships between seasonality, circadian misalignment, and shift work adaptation. Our analyses show that seasonal variations corresponding to changes in day length are associated with day-to-day circadian misalignment. In our dual oscillator model, the mechanisms involved in seasonal timing also modulate circadian entrainment. In addition, we found significant differences in daily steps, time awake, and HR-sleep misalignment throughout the year across different genotypes, grouped by polymorphisms of the *SLC20A2* gene. We see much larger differences in HR-sleep misalignment between the genotype groups in the winter than in the summer. Based on these findings, we hypothesize that *SLC20A2* influences photoperiodic encoding in humans.

It is thought that the circadian phase difference between the core and shell regions of the SCN is involved in photoperiodic encoding, with these regions acting as “evening” and “morning” oscillators. Previous models of seasonal timing make the simplification that only the SCN core receives light signaling<sup>43,55,56</sup>. In simulations, seasonal changes are then created by artificially adjusting the neuronal coupling strength based on photoperiod, but this approach does not explain *how* the SCN detects photoperiod. Our model is novel in that it assumes both regions of the SCN receive light signaling, which is supported by experiments<sup>57</sup>. At the same time, their phases are naturally pushed away from each other due to different intrinsic



frequencies. In our dual circadian oscillator model, circadian timekeeping can depend on the strength of light signaling in either oscillator as well as the coupling between the two oscillators. Our mathematical model shows strong evidence that the inter-individual differences in circadian timekeeping could be explained by altered light signaling in the evening oscillator or coupling between the oscillators. The differences in the parameters shown in Fig. 5b, c are small but statistically significant. For all 7 parameters, we chose to omit outliers more than three scaled MAD from the median. For some of the outlier parameters, we found that the ODE model has irregular dynamics, including phase drifting or bursting-like behaviors. We plan to investigate these dynamics in future work.

Genotype group 9 exhibited the largest HR-sleep misalignment, yet our ODE model predicts that this group also demonstrates strong E-to-M coupling and robust circadian entrainment to 12-hour phase shifts. We also find in the data that this group responds quickly to night shifts (Fig. 6). Although counterintuitive, this pattern likely arises because medical interns primarily work day shifts with occasional night shifts. The circadian clock adjusts slowly, so a few night shifts after many day shifts don't cause major misalignment if the clock hasn't fully shifted. However, if it entrains quickly (e.g. for group 9), one or two night shifts can lead to greater misalignment after switching back to day shifts. In this dataset, most of the night shifts were 1-3 consecutive night shifts. Various jet lag and shift work disorder treatment approaches aim to speed up entrainment of circadian rhythms to external cues<sup>58</sup>. For long periods of consecutive night shifts, we expect that quick entrainment will instead lead to lower misalignment on average, but the behavior for frequent, short periods of schedule changes is less intuitive. Previous mathematical models have previously explored the effects of melatonin treatment<sup>59</sup> and light exposure therapy<sup>60</sup> on the circadian clock as a single-oscillator system. Our ODE model can be used to further investigate the effects of shift schedules and altered seasonal timing mechanisms on shiftwork adaptation.

It is well established that *Drosophila*, rodents, and other crepuscular animals with morning and evening bouts of activity have populations of neurons in the SCN that track dawn and dusk. In humans, the onset of melatonin secretion occurs around dusk, and the offset occurs around dawn<sup>61</sup>. While there may not be any noticeable inter-individual differences in circadian timekeeping during regular, 24 h-periodic light-dark conditions, individual responses to schedule changes can vary tremendously. Based on our findings, we hypothesize that *SLC20A2*, localized in SCN core neurons and involved in seasonal timing in mice<sup>33</sup>, may be involved in seasonal timing in humans as well, influencing shiftwork adaptation. While statistically significant, the combined effects of the *SLC20A2* SNPs in our study are quite small and complex—small effect sizes are expected in genetic contributions to human behavior<sup>62</sup>. We do not think that *SLC20A2* alone can explain differences in seasonal behaviors and shiftwork adaptation, but it may contribute as one of many genetic factors influencing inter-individual variability. Further studies are needed to clarify the role of *SLC20A2* in the biological pathways regulating seasonal timing in humans and how these pathways influence circadian entrainment. In addition, studies at the intersection of work, individual differences, and genetics require careful interpretation<sup>63</sup>. Importantly, our findings do not speak to how well individuals perform during their shifts and should not be used to make assumptions about capability or performance.

We show that there is a relationship between seasonal timing and shiftwork adaptation, but the relationship is not straightforward and can be influenced by many other external factors. Some individuals have more circadian misalignment on average due to quick responses to abrupt schedule changes, but in some cases this may be advantageous. Understanding these differences will allow for a deeper understanding of circadian and seasonal timing as well as their health impacts. Our study shows strong evidence for a contributing role of photoperiodic timing in shiftwork adaptation, and we believe that these effects may extend to other modern-day challenges (e.g., east-west travel) as well.

Genetic polymorphisms linked to speeding up or slowing down intracellular timing can affect overall circadian rhythms, and even our ability

to adjust to daylight saving time<sup>64</sup>. To our knowledge, our study is the first to explore the effects of seasonality and genetics on shift work adaptation in humans. Our study contributes several new insights related to human circadian rhythms. Despite mixed findings in the literature, our findings use data from real-world settings to corroborate previous studies showing statistically significant seasonal effects in humans. Our study suggests that HR-sleep misalignment can be caused by seasonal encoding mechanisms that are tracking day-to-day schedule changes in a modern-day context. In addition, we found that there were statistically significant effects of *SLC20A2* SNPs on daily steps, HR-sleep misalignment, and time awake throughout the year, and using a mathematical model, we studied inter-individual differences in seasonal timing and shiftwork adaptation. We believe that our findings have important implications for shift work, suggesting that heightened sensitivity to seasonal cues may contribute to circadian misalignment in response to irregular schedules. These insights highlight the need for personalized strategies in managing shift work to mitigate potential health risks associated with circadian disruption.

## Methods

### Study design and participants

Two to three months before the start of the internship, incoming interns were invited via email to participate. The interns who consented then completed a baseline (pre-internship) survey. Saliva samples were collected via mail. Participants were provided a Fitbit Charge 2 or Inspire HR to collect sleep, steps, and heart rate data; or \$50 if they already had a compatible Fitbit (Fitbit Inc., San Francisco, CA). The University of Michigan Institutional Review Board approved the study, and all subjects provided informed consent after receiving a complete description of the study.

### Genotyping

Interns provided saliva samples using the Oragene salivary DNA kits<sup>65</sup>. The Illumina Infinium CoreExome-24+ Chip was used for genotyping for the IHS sample. Next, quality check was implemented by removing samples with call rate <99%, a sex mismatch between genotype data and reported data, or a lower call rate when duplicated, and removing SNPs with call rate <98% (after sample removal) and minor allele frequency (MAF) <0.005. Linkage disequilibrium (LD) based SNP pruning was then performed with a window size of 100 kilobases (kb), a step size of 25 variants, and pairwise  $r^2$  threshold 0.5. Finally, top 10 principal components (PCs) were extracted from the genotyped data based on the variance-standardized relationship matrix. Quality check, LD-pruning, and PCs extraction were all performed with PLINK v.1.9<sup>66</sup>.

### *SLC20A2* variant extraction

We used R package 'rentrez' [`<rentrez>`], which works with the NCBI Entrez Programming Utilities (E-utilities) API to search data from NCBI databases, to isolate all *SLC20A2* SNPs from the genotyped data. From the variants genotyped in our sample, we found 6 single-nucleotide polymorphisms (SNPs) of *SLC20A2* (rs3763510, rs34749433, rs4737046, rs6988483, rs13281070, and rs7818789), of which 5 (excluding rs7818789) were not in LD and effectively independent of each other in terms of inheritance.

### Bowman Algorithm

The Bowman algorithm<sup>24</sup> is used to determine the phase of HR circadian rhythms from heart rate and activity data. The model for HR at hour  $t$  is given by

$$HR_t = a - b \cos\left(\frac{\pi}{12}(t - c)\right) + d \cdot \text{Activity} + \epsilon_t, \quad (1)$$

with parameters  $a$ ,  $b$ ,  $c$ , and  $d$ , and an error term. HR increases proportionally to activity (steps), and the time of the HR minimum ( $c$ ) is taken as the circadian phase. In this study, the consumer wrist-worn Fitbit Charge 2 was used to continuously collect heart rate, sleep, and activity data from medical interns. A validation study of the Fitbit Charge 2 compared to gold

standard polysomnography showed a sensitivity of 0.96 (accuracy in detecting sleep) and a specificity of 0.61 (accuracy in detecting wake) in healthy adults<sup>67</sup>. Other studies support the sufficient accuracy of the Fitbit Charge 2 in measuring heart rate<sup>68</sup>. Another study<sup>69</sup> has shown that wrist-worn wearable devices measuring heart rate perform well at rest but can have limited accuracy during exercise. The concordance correlation coefficient for Fitbit Charge HR (part of the same Charge series) against electrocardiogram was 0.84. In addition, there are many external factors influencing heart rate, including meals<sup>70</sup> and stress<sup>71</sup>. Noise accounting for these effects is modeled as Gaussian noise plus an AR(1) process,

$$\epsilon_{t+1} = k\epsilon_t + N(0, \sigma^2) \quad (2)$$

Parameters are estimated via Goodman and Weare's affine-invariant Markov chain Monte Carlo algorithm<sup>72</sup>. More details about the model and parameter estimation can be found in the original paper<sup>24</sup> and the code used is publicly available at <https://github.com/pepperhuang/heartate>.

### Dual oscillator mathematical model

The model in this paper consists of two ordinary differential equations (ODEs) describing the rate of change of the phases of two oscillators, the evening (E) and morning (M) oscillators. The oscillators are coupled to each other and to a light signal, where synchronization rates depend on the phase difference with the synchronizing oscillator (E, M, or light). A schematic diagram is provided in Fig. 2a and the ODEs are given by

$$\dot{\phi}_E = \omega_E + A_E \sin(\phi_M - \phi_E) + A_{ZE}(L) \sin(\phi_L - \phi_E), \quad (3)$$

$$\dot{\phi}_M = \omega_M + A_M \sin(\phi_E - \phi_M) + A_{ZM}(L) \sin(\phi_L - \phi_M), \quad (4)$$

where  $\omega_E = \frac{2\pi}{24+D_E(L)}$ ,  $\omega_M = \frac{2\pi}{24+D_M(L)}$ , and

$$\phi_L(t) = \begin{cases} \frac{\pi t}{L}, & t < L \\ \frac{\pi(t-L)}{24-L} + \pi, & t \geq L \end{cases} \quad (5)$$

$\phi_E$  and  $\phi_M$  are the phases of the E and M oscillators, respectively, and  $t$  is in hours.  $\omega_E$  and  $\omega_M$  represent intrinsic frequencies. The second term in each of Eqs. (3) and (4) describes the coupling effect of the other (E or M) oscillator, and the third term describes the effect of light signaling. The phase of the light oscillator with photoperiod  $L$  is denoted  $\phi_L$  (Eq. (5)). Here,  $\phi_L(0) = \phi_L(24) = 0$  radians so that the light signal is 24 h periodic and  $\phi_L(L) = \pi$  radians so that the oscillator completes half a cycle at the end of the light phase. Light signaling drives their intrinsic frequencies further apart as in ref. 8. We take this effect to be sigmoidal, where  $D_i(L) = (1 + \exp(-p(a_i L - 1)))^{-1}$  for  $i \in \{E, M\}$ . The light intensity is represented by  $a_i L$  so that it is proportional to the photoperiod, as it is in natural settings. The functions  $A_{ZE}(L) = a_e b_e L$  and  $A_{ZM}(L) = a_m b_m L$  account for light intensity  $a_e L$  and  $a_m L$  and coupling strength through the parameters  $b_e$  and  $b_m$ . For each participant, we took  $L$  to be the natural photoperiod at their geographic location. Sunlight is significantly brighter than indoor lighting, and several studies show that even when individuals spend most of their time indoors, they are exposed to bright light throughout the day in relation to day length<sup>73–75</sup>.

The initial parameter values used for nonlinear least-squares fitting were  $a_e = 0.0833$ ,  $a_m = 0.0833$ ,  $b_e = 0.009$ ,  $b_m = 0.008$ ,  $A_e = 0.001$ ,  $A_m = 0.001$ , and  $p = 2.5$ . These values were informed by simulations in previous studies using a dual oscillator model<sup>43,44</sup>. Before fitting, the data was normalized by the group 1 average (8,742.7 steps) and the phase gap curves were normalized by 4.35 h so that the normalized group 1 phase gaps were centered around 1 (see Fig. 5a). In comparing parameter values across groups, we omitted parameters beyond 3 scaled median absolute deviations (MAD) from the median, which corresponded to about 10% from both the upper and lower ends of each set on average. This threshold was applied symmetrically and consistently across groups. Numerical solutions for the ODEs were computed using ode45 in MATLAB. The

code for the ODEs and parameter fitting is provided at [https://github.com/rubyshkim/twophase\\_ODEs](https://github.com/rubyshkim/twophase_ODEs).

### Data availability

The de-identified data from Intern Health Study that supports our findings are available from the authors upon reasonable request.

### Code availability

The MATLAB code for the mathematical model is available at [https://github.com/rubyshkim/twophase\\_ODEs](https://github.com/rubyshkim/twophase_ODEs). The code created for the data analyses in this paper is available from the authors upon reasonable request.

Received: 17 February 2025; Accepted: 25 April 2025;

Published online: 28 May 2025

### References

- Samson, D. R. & McKinnon, L. Are humans facing a sleep epidemic or enlightenment? large-scale, industrial societies exhibit long, efficient sleep yet weak circadian function. *Proc. B* **292**, 20242319 (2025).
- Schmid, S. R. et al. How smart is it to go to bed with the phone? the impact of short-wavelength light and affective states on sleep and circadian rhythms. *Clocks Sleep*. **3**, 558–580 (2021).
- Jackson, S. D. Plant responses to photoperiod. *N. Phytol.* **181**, 517–531 (2009).
- Hut, R. A. & Beersma, D. G. Evolution of time-keeping mechanisms: early emergence and adaptation to photoperiod. *Philos. Trans. R. Soc. B: Biol. Sci.* **366**, 2141–2154 (2011).
- Wehr, T. A. In short photoperiods, human sleep is biphasic. *J. Sleep. Res.* **1**, 103–107 (1992).
- Wehr, T. A. et al. Conservation of photoperiod-responsive mechanisms in humans. *Am. J. Physiol. -Regul., Integr. Comp. Physiol.* **265**, R846–R857 (1993).
- Wang, Q., Liu, W., Leung, C. C., Tarté, D. A. & Gendron, J. M. Plants distinguish different photoperiods to independently control seasonal flowering and growth. *Science* **383**, eadg9196 (2024).
- Pittendrigh, C. S. & Daan, S. A functional analysis of circadian pacemakers in nocturnal rodents. *J. Comp. Physiol.* **106**, 333–355 (1976).
- Hoffmann, K. Splitting of the circadian rhythm as a function of light intensity. *Biochronometry* **134**, 50 (1971).
- Yoshii, T., Rieger, D. & Helfrich-Förster, C. Two clocks in the brain: an update of the morning and evening oscillator model in *Drosophila*. *Prog. Brain Res.* **199**, 59–82 (2012).
- Collins, B. et al. Circadian VIPergic neurons of the suprachiasmatic nuclei sculpt the sleep-wake cycle. *Neuron* **108**, 486–499.e5 (2020).
- Saini, R., Jaskolski, M. & Davis, S. J. Circadian oscillator proteins across the kingdoms of life: structural aspects. *BMC Biol.* **17**, 1–39 (2019).
- Schwartz, W. J., Reppert, S. M., Eagan, S. M. & Moore-Ede, M. C. In vivo metabolic activity of the suprachiasmatic nuclei: a comparative study. *Brain Res.* **274**, 184–187 (1983).
- Bell-Pedersen, D. et al. Circadian rhythms from multiple oscillators: lessons from diverse organisms. *Nat. Rev. Genet.* **6**, 544–556 (2005).
- Evans, J. A. & Schwartz, W. J. On the origin and evolution of the dual oscillator model underlying the photoperiodic clockwork in the suprachiasmatic nucleus. *J. Comp. Physiol. A* **210**, 503–511 (2024).
- Wehr, T. A. The durations of human melatonin secretion and sleep respond to changes in (photoperiod). *J. Clin. Endocrinol. Metab.* **73**, 1276–1280 (1991).
- Wehr, T. A. Photoperiodism in humans and other primates: evidence and implications. *J. Biol. Rhythms* **16**, 348–364 (2001).
- Wright, K. P. et al. Entrainment of the human circadian clock to the natural light-dark cycle. *Curr. Biol.* **23**, 1554–1558 (2013).

19. Dunster, G. P. et al. Daytime light exposure is a strong predictor of seasonal variation in sleep and circadian timing of university students. *J. Pineal Res* **74**, e12843 (2023).
20. Mattingly, S. M. et al. The effects of seasons and weather on sleep patterns measured through longitudinal multimodal sensing. *npj Digit. Med.* **4**, 76 (2021).
21. Li, L., Nakamura, T., Hayano, J. & Yamamoto, Y. Seasonal sleep variations and their association with meteorological factors: a Japanese population study using large-scale body acceleration data. *Front. Digit. Health* **3**, 677043 (2021).
22. Turrise, T. B. et al. Seasons, weather, and device-measured movement behaviors: a scoping review from 2006 to 2020. *Int. J. Behav. Nutr. Phys. Act.* **18**, 24 (2021).
23. Moreno, J. P. et al. Potential circadian and circannual rhythm contributions to the obesity epidemic in elementary school age children. *Int. J. Behav. Nutr. Phys. Act.* **16**, 1–10 (2019).
24. Bowman, C. et al. A method for characterizing daily physiology from widely used wearables. *Cell Rep. Methods* **1**, 8 (2021).
25. Kim, D. W., Lee, M. P. & Forger, D. B. Wearable Data Assimilation to Estimate the Circadian Phase. *SIAM J. Appl. Math.* **84**, S452–S475 (2024).
26. Kim, D. W. et al. Efficient assessment of real-world dynamics of circadian rhythms in heart rate and body temperature from wearable data. *J. R. Soc. Interface* **20**, 20230030 (2023).
27. Gamble, K. L. et al. Shift work in nurses: Contribution of phenotypes and genotypes to adaptation. *PLOS ONE* **6**, 1–12 (2011).
28. Li, X. & Zhao, H. Automated feature extraction from population wearable device data identified novel loci associated with sleep and circadian rhythms. *PLOS Genet.* **16**, 1–22 (2020).
29. Cui, S. et al. Care as a wearable derived feature linking circadian amplitude to human cognitive functions. *npj Digit. Med.* **6**, 123 (2023).
30. Ho, K. W. D. et al. Genome-wide association study of seasonal affective disorder. *Transl. Psychiatry* **8**, 190 (2018).
31. Li, P., Guo, M., Wang, C., Liu, X. & Zou, Q. An overview of SNP interactions in genome-wide association studies. *Brief. Funct. Genom.* **14**, 143–155 (2014).
32. Garbaza, C. & Benedetti, F. Genetic factors affecting seasonality, mood, and the circadian clock. *Front. Endocrinol.* **9**, 481 (2018).
33. Pierre-Ferrer, S. et al. A phosphate transporter in VIPergic neurons of the suprachiasmatic nucleus gates locomotor activity during the light/dark transition in mice. *Cell Rep.* **43**, 114220 (2024).
34. Wiens, T. Day length. <https://www.mathworks.com/matlabcentral/fileexchange/20390-day-length>, 2015. [Online; accessed February 12, 2024].
35. Vetter, C. Circadian disruption: What do we actually mean?. *Eur. J. Neurosci.* **51**, 531–550 (2020).
36. Snyder, F., Hobson, J. A., Morrison, D. F. & Goldfrank, F. Changes in respiration, heart rate, and systolic blood pressure in human sleep. *J. Appl. Physiol.* **19**, 417–422 (1964).
37. Morris, C. J., Purvis, T. E., Hu, K. & Scheer, F. A. J. L. Circadian misalignment increases cardiovascular disease risk factors in humans. *Proc. Natl. Acad. Sci. USA* **113**, E1402–E1411 (2016).
38. Lee, M. P. et al. The real-world association between digital markers of circadian disruption and mental health risks. *NPJ Digit. Med.* **7**, 1–15 (2024).
39. Fudolig, M. I. et al. The two fundamental shapes of sleep heart rate dynamics and their connection to mental health in college students. *Digit. Biomark.* **8**, 120–131 (2024).
40. Ratcliffe, S. J. & Shults, J. GEEQBOX: A MATLAB toolbox for generalized estimating equations and quasi-least squares. *J. Stat. Softw.* **25**, 1â€14 (2008).
41. Price, A. L. et al. Principal components analysis corrects for stratification in genome-wide association studies. *Nat. Genet.* **38**, 904–909 (2006).
42. Honma, K., Honma, S., Kohsaka, M. & Fukuda, N. Seasonal variation in the human circadian rhythm: dissociation between sleep and temperature rhythm. *Am. J. Physiol.* **262**, R885–R891 (1992).
43. Myung, J. et al. Gaba-mediated repulsive coupling between circadian clock neurons in the SCN encodes seasonal time. *Proc. Natl. Acad. Sci. USA* **112**, E3920–E3929 (2015).
44. Myung, J. & Pauls, S. D. Encoding seasonal information in a two-oscillator model of the multi-oscillator circadian clock. *Eur. J. Neurosci.* **48**, 2718–2727 (2018).
45. Schmal, C., Herzog, E. D. & Herzog, H. Measuring relative coupling strength in circadian systems. *J. Biol. Rhythms* **33**, 84–98 (2018).
46. Lynch, H. J. et al. Entrainment of rhythmic melatonin secretion in man to a 12-hour phase shift in the light/dark cycle. *Life Sci.* **23**, 1557–1563 (1978).
47. Mills, J., Minors, D. & Waterhouse, J. Adaptation to abrupt time shifts of the oscillator (s) controlling human circadian rhythms. *J. Physiol.* **285**, 455–470 (1978).
48. Diekman, C. O. & Bose, A. Beyond the limits of circadian entrainment: Non-24-h sleep-wake disorder, shift work, and social jet lag. *J. Theor. Biol.* **545**, 111148 (2022).
49. Monsivais, D., Bhattacharya, K., Ghosh, A., Dunbar, R. I. & Kaski, K. Seasonal and geographical impact on human resting periods. *Sci. Rep.* **7**, 10717 (2017).
50. Walker, N. J., Van Woerden, H. C., Kiparoglou, V. & Yang, Y. Identifying seasonal and temporal trends in the pressures experienced by hospitals related to unscheduled care. *BMC Health Serv. Res.* **16**, 1–10 (2016).
51. Suhail, K. & Cochrane, R. Seasonal variations in hospital admissions for affective disorders by gender and ethnicity. *Soc. Psychiatry Psychiatr. Epidemiol.* **33**, 211–217 (1998).
52. Akintoye, E. et al. Seasonal variation in hospitalization outcomes in patients admitted for heart failure in the United States. *Clin. Cardiol.* **40**, 1105–1111 (2017).
53. Lewy, A. J. Circadian misalignment in mood disturbances. *Curr. Psychiatry Rep.* **11**, 459–465 (2009).
54. Sandman, N. et al. Winter is coming: nightmares and sleep problems during seasonal affective disorder. *J. Sleep. Res.* **25**, 612–619 (2016).
55. DeWoskin, D. et al. Distinct roles for GABA across multiple timescales in mammalian circadian timekeeping. *Proc. Natl. Acad. Sci.* **112**, E3911–E3919 (2015).
56. Hannay, K. M., Forger, D. B. & Booth, V. Seasonality and light phase-resetting in the mammalian circadian rhythm. *Sci. Rep.* **10**, 19506 (2020).
57. Fernandez, D. C., Chang, Y.-T., Hattar, S. & Chen, S.-K. Architecture of retinal projections to the central circadian pacemaker. *Proc. Natl. Acad. Sci.* **113**, 6047–6052 (2016).
58. Zee, P. C. & Goldstein, C. A. Treatment of shift work disorder and jet lag. *Curr. Treat. Options Neurol.* **12**, 396–411 (2010).
59. Best, J., Kim, R., Reed, M. & Nijhout, H. F. A mathematical model of melatonin synthesis and interactions with the circadian clock. *Math. Biosci.* **377**, 109280 (2024).
60. Serkh, K. & Forger, D. B. Optimal schedules of light exposure for rapidly correcting circadian misalignment. *PLoS Comput. Biol.* **10**, e1003523 (2014).
61. Arendt, J. Melatonin and human rhythms. *Chronobiol. Int.* **23**, 21–37 (2006).
62. Chabris, C. F., Lee, J. J., Cesarini, D., Benjamin, D. J. & Laibson, D. I. The fourth law of behavior genetics. *Curr. Direct. Psychol. Sci.* **24**, 304–312 (2015).
63. Martschenko, D. O. Ethics of genomic research on occupational status. *Nat. Hum. Behav.* **9**, 245–247 (2025).
64. Tyler, J. et al. Genomic heterogeneity affects the response to daylight saving time. *Sci. Rep.* **11**, 14792 (2021).
65. Rogers, N. L., Cole, S. A., Lan, H.-C., Crossa, A. & Demerath, E. W. New saliva DNA collection method compared to buccal cell collection

- techniques for epidemiological studies. *Am. J. Hum. Biol.* **19**, 319–326 (2007).
66. Chang, C. C. et al. Second-generation PLINK: rising to the challenge of larger and richer datasets, *GigaScience* **4**, s13742–015–0047–8, 02 (2015).
  67. De Zambotti, M., Goldstone, A., Claudatos, S., Colrain, I. M. & Baker, F. C. A validation study of Fitbit Charge 2<sup>®</sup> compared with polysomnography in adults. *Chronobiol. Int.* **35**, 465–476 (2018).
  68. Irwin, C. & Gary, R. Systematic review of Fitbit Charge 2 validation studies for exercise tracking. *Transl. J. Am. Coll. Sports Med.* **7**, 1–7 (2022).
  69. Wang, R. et al. Accuracy of wrist-worn heart rate monitors. *JAMA Cardiol.* **2**, 104–106 (2017).
  70. Young, H. A. & Benton, D. Heart-rate variability: a biomarker to study the influence of nutrition on physiological and psychological health?. *Behav. Pharmacol.* **29**, 140–151 (2018).
  71. Kim, H.-G., Cheon, E.-J., Bai, D.-S., Lee, Y. H. & Koo, B.-H. Stress and heart rate variability: a meta-analysis and review of the literature. *Psychiatry Investig.* **15**, 235 (2018).
  72. Goodman, J. & Weare, J. Ensemble samplers with affine invariance. *Commun. Appl. Math. Comput. Sci.* **5**, 65–80 (2010).
  73. Hubert, M., Dumont, M. & Paquet, J. Seasonal and diurnal patterns of human illumination under natural conditions. *Chronobiol. Int.* **15**, 59–70 (1998).
  74. Dumont, M. & Beaulieu, C. Light exposure in the natural environment: relevance to mood and sleep disorders. *Sleep. Med.* **8**, 557–565 (2007).
  75. Thorne, H. C., Jones, K. H., Peters, S. P., Archer, S. N. & Dijk, D.-J. Daily and seasonal variation in the spectral composition of light exposure in humans. *Chronobiol. Int.* **26**, 854–866 (2009).

## Acknowledgements

The authors gratefully acknowledge funding from MURI through the ARO W911NF-22-1-0223, NIMH R0101459, and NSF DMS grant 2052499, the National Research Foundation of Korea RS-2025-00561696, and the KAIST start-up research fund G04240060.

## Author contributions

R.K. was involved in study conception and design, performed computational simulations, analyzed the data, contributed to data interpretation, prepared the figures, and wrote the manuscript draft. Y.F. extracted the data, contributed to data interpretation, and contributed to writing the Methods. M.P.L. curated the data, performed computational simulations, and contributed to data interpretation. D.W.K. curated the data and contributed

to data interpretation. Z.T. contributed to data interpretation. S.S. was involved in study conception and design and contributed to data interpretation. D.B.F. was involved in study conception and design, contributed to data interpretation, and contributed to writing. All authors have read and approved the final manuscript.

## Competing interests

DBF is the CSO of Arcascope, a company that makes circadian rhythms software. Both he and the University of Michigan are part owners of Arcascope. Arcascope did not sponsor this research. All other authors declare they have no competing interests.

## Additional information

**Supplementary information** The online version contains supplementary material available at <https://doi.org/10.1038/s41746-025-01678-z>.

**Correspondence** and requests for materials should be addressed to Ruby Kim or Daniel B. Forger.

**Reprints and permissions information** is available at <http://www.nature.com/reprints>

**Publisher's note** Springer Nature remains neutral with regard to jurisdictional claims in published maps and institutional affiliations.

**Open Access** This article is licensed under a Creative Commons Attribution-NonCommercial-NoDerivatives 4.0 International License, which permits any non-commercial use, sharing, distribution and reproduction in any medium or format, as long as you give appropriate credit to the original author(s) and the source, provide a link to the Creative Commons licence, and indicate if you modified the licensed material. You do not have permission under this licence to share adapted material derived from this article or parts of it. The images or other third party material in this article are included in the article's Creative Commons licence, unless indicated otherwise in a credit line to the material. If material is not included in the article's Creative Commons licence and your intended use is not permitted by statutory regulation or exceeds the permitted use, you will need to obtain permission directly from the copyright holder. To view a copy of this licence, visit <http://creativecommons.org/licenses/by-nc-nd/4.0/>.

© The Author(s) 2025